1. Title page

Elastic modulus of woven bone: correlation with evolution of porosity and x-ray greyscale.

J. Mora-Macías[1], P García-Florencio[2], A. Pajares[3], P. Miranda[3], J. Domínguez[2], E. Reina-Romo[2]

[1] University of Huelva. Department of Mining, Mechanical, Energy and Construction Engineering. Huelva (Spain).

[2] University of Seville. Department of Mechanical and Manufacturing Engineering. Seville (Spain).

[3] Department of Mechanical, Energy and Materials Engineering, University of Extremadura, Badajoz (Spain).

Corresponding author: Juan Mora Macías. Email: juan.mora@dimme.uhu.es Phone: +34 959217322

2. Abstract and key terms

The woven bone created during the healing of bone regeneration processes is characterized as being extremely inhomogeneous and having a variable stiffness that increases with time. Therefore, it is important to study how the mechanical properties of woven bone are dependent on its microarchitecture and especially on its porosity and mineral content. The porosity and the x-ray greyscale of specimens taken from bone transport studies in sheep were assessed by means of *ex vivo* imaging. Our study demonstrates that the porosity of the woven bone in the distraction area diminishes during the healing process from 73.3% 35 days after surgery to 31.9% 525 days after surgery. In addition, the woven bone's porosity is negatively correlated with its Young's modulus. The x-ray greyscale, was measured as an indicator of the level of mineralisation of the woven bone. Greyscale index has been demonstrated to be inversely proportional to porosity and to increase to up to 60-80% of the level in cortical bone. The results of this study may contribute to the development of micromechanical models of woven bone and improvements in *in silico* modelling.

Key words: porosity, greyscale, x-ray, mineralisation, elastic modulus, pore area, woven bone, bone transport.

3. Introduction

Many orthopaedic treatments, such as fractures or segmental bone defects, depend on the generation of new bone tissue or woven bone. Orthopaedic treatments associated to bone regeneration processes consume a large amount of resources of the health systems in most countries in the world, affect many patients and not all of them end successfully. For example, infection or non-union may affect at least 5% of complex tibial fractures[15], subsequently require treatment of tibial defects. In general, segmental bone loss occurs at 0.4% of all fractures[34]. It implies that yearly over two million people need a segmental bone defect treatment worldwide, with costs around US $3 billion every year[39]. One of the techniques used in the treatment of segmental bone defects is bone transport[4] which consists of applying distraction osteogenesis[17,18]. In the case of femoral distraction osteogenesis, this type of interventions have a cost around US $50,000[36].

Distraction osteogenesis is a very complex process which poses numerous challenges. Good judgement, accurate knowledge and meticulous techniques are necessary for selecting and designing devices, performing corticotomies, maximising bone regeneration, managing pin sites, maintaining articular function and timing fixator removal[13]. Bone transport presents two sites at which woven bone develops: the distraction callus and the docking site. As the woven bone generated during the healing process needs to extend to areas without bone, it is quickly formed and poorly organised and is characterised as having a variable stiffness that increases with time[28,31]. As its structure evolves, the composition[26] and mechanical properties also consequently change[32]. Therefore, it is important to study how the mechanical properties of woven bone are dependent on its microarchitecture and especially on its porosity and degree of mineralisation.

The porosity of cortical bone has been widely studied. In a recent review, Currey and Shahar[12] identified five levels of porosity, namely (from large to small) (1) the marrow cavity, (2) channels for the nutrient arteries that traverse the cortex, (3) vascular porosity within the cortex, (4) lacunar-canalicular porosity, and the (5) 'nanoporosity' between the collagen and the hydroxyapatite crystals. Apart from the central medullary cavity, these channels do not result in a high porosity, 10% at most[12]. It has been demonstrated that the mechanical properties of cortical bone depend on its porosity[9,25,27,38,40]. In fact, high cortical porosity has been negatively associated with bone stiffness, toughness and elasticity, as well as impact energy absorption capacity[2,8,9,11,38]. The elastic modulus of the cortical bone is related to porosity to the 10.9th power[38]; accordingly, a change in porosity from 10% to 15% results in a 46% reduction in the cortical bone's elastic modulus. Studies conducted on trabecular bone point to it having a porosity between 70-95%[35,38]. There is no significant correlation between the porosity of cortical bone and the porosity of trabecular bone[35].

There have also been studies on mineral content in both cortical and trabecular bone[9,16,22,24,35]. The mineral content of trabecular bone, studied in vertebrate animals, was approximately 95% of the mineral content of cortical bone[9,16]. Currey[9] calculated the amount of calcium in dehydrated bone using a colorimetric method, relating the Young's modulus to the degree of mineralisation of the cortical. Currey[10] showed that low mineral content in the bone caused it to have a lower elastic modulus than a bone with high mineral content. Renders et al.[35] calculated the mineral content of both cortical and trabecular bone, finding that the degree of mineralisation of trabecular bone was much lower than that of cortical bone during the process of creating new bone.

However, there seems to be little published work on measurements of the porosity and mineralisation of woven bone. The properties of the tissues have been analysed in most

cases at a macroscopic and microscopic level[24]. To assess the degree of mineralisation, computed tomography[22,40], dual-energy X-ray absorptiometry (DEXA) [1], or backscattered electron imaging (qBEI)[24,37] have been used. This last technique allows for the determination of the calcium content from backscattered electron microscope images. The macroscopic mechanical properties of woven bone have been analysed *ex vivo*[14], *in vivo*[6,28-30] and *in silico*[33,40]. For example, Mora-Macías et al.[32] and Manjubala et al.[24] have evaluated the temporal and spatial variations of woven bone during both bone transport and fracture healing calluses respectively using nanoindentation measurements. In addition, Manjubala et al[24], correlated the mineral content and the nanoindentation modulus for woven bone during fracture healing. Vetter et al.[41] also reported the evolution of the porosity of the woven bone in fracture healing.

The measurement of the porosity and mineral content of woven bone can be of enormous value for *in silico* models[44]. Table 1 shows the values for porosity used in mechanobiological models found in the literature on fracture healing and distraction osteogenesis[5,19-21]. As can be observed, a value of 80% is typically assigned to woven bone, while 4% is selected for cortical bone. It must be highlighted that the value of 80% used in these works is not taken from any experimental study, which highlights the necessity of experimentally measuring the porosity of woven bone. Furthermore, Vetter et al.[42] and Mora-Macías et al.[33] demonstrate the influence of taking into account the woven bone porosity in *in silico* studies. The former showed, differences in the strain field of a fracture callus between a computational model that takes into account the heterogeneity of the woven bone and another that considers the callus to be homogenous, once bony bridge is reached. Similarly, Mora-Macías et al.[33] showed that correlation with experimental results is not possible after bony bridging if homogeneous callus and

constant porosity are assumed in an *in silico* model of distraction osteogenesis. Stiffness of the callus reported by this model was compared against reported *in vivo* results[28]

Table 1: Values for the porosity and Young's modulus (E) of the woven and cortical bone used in mechanobiological models.

To the best of the authors' knowledge, no direct measurement of porosity has yet been carried out in woven bone generated during distraction osteogenesis. Also, no correlation of the stiffness of the callus with mineralisation and porosity has ever been made. Consequently, the overall goals of this study are: (1) to quantify the temporal evolution of the porosity of the woven bone throughout the distraction callus; (2) to evaluate its relative x-ray greyscale with reference to cortical bone greyscale, as a qualitative indicator of the level of mineralisation; and (3) to investigate the relationships between these two variables (porosity and greyscale) and the Young's modulus of the woven bone.

4. Materials and methods

Bone transport experiment

The bone transport experiment was performed using 11 Merino sheep, aged between 3 and 5 years, with an average weight of 53±8.5 kg[28]. Bone transport was applied in the metatarsus of the right hind limb, where the distraction callus was generated during 15 days (1mm/day). During the experiments, the welfare of each of the sheep was guaranteed according to the regulations of the Research Ethics Committee of the University of Seville. The animals in the experiment in question were euthanized at different stages of the bone transport process to obtain *ex vivo* samples of the distraction callus.

To analyse the evolution of the porosity, 6 callus samples in which most of the tissue had been ossified were used (one per animal and time point, sheep were euthanised at days

35, 50, 79, 98, 161 and 525 after surgery). Specimens were prepared as in a previous study[32], in which the same samples were used to measure the elastic modulus via nanoindentation. For each callus sample, a sheet 2 mm thick was extracted from the surface parallel to the frontal plane of the limb (Fig. 1a). The sheets of callus tissue were embedded in an Epofix® (Struers, California, US) resin cylinder (25 mm in diameter and 25 mm in height). The surface of the samples was polished with carbide papers (P600 to P4000) and diamond slurry (from 3 to 0.25 μm). Colloidal silica slurry (0.04 μm) was used for the final polishing step. The specimens were ultrasonically cleaned with distilled water between each polishing step. An instance of a sample obtained at the end of the process described, corresponding to a specimen harvested 35 days after surgery, is shown in Fig. 1c. For each specimen, a digital image was taken through an optical microscope (micrograph) from the distraction callus area (Figs. 2a, 2b and 2c). Since one animal was euthanised per time-point, a total of 6 micrographs were obtained. In addition, for each animal, a cortical bone sample from the proximal bone segment was also considered and equally processed for control measurements (Figs. 1b and 1d).

Fig. 1.Location of the (a) distraction callus and (b) cortical bone samples within the cross section (parallel to frontal plane) of the intervened metatarsus. Photographs shown in (c) and (d) correspond to the distraction callus and cortical bone samples respectively, taken from the sheep sacrificed at day 79 after surgery.

To analyse the evolution of the x-ray greyscale of the distraction callus, radiographs of the 11 sheep were taken periodically *in vivo*, from initial surgery to slaughter, or the end of the intervention. In total, 172 radiographs were taken on two distinct planes, mediolateral and dorsoplantar, and at different time points after surgery (Table 2). Radiographs were taken weekly from surgery to one month after surgery, then every two weeks until 6 months after surgery, then monthly from 6 months after surgery (Table 2).

Table 2. Time points at which radiographs were taken of each of the 11 sheep in the study

Estimation of porosity

For the quantification of the porosity throughout the entire distraction process, 6 micrographs (one per specimen and sacrifice time-point) of the distraction callus were analysed through image processing with Matlab®. The process followed to estimate the porosity is illustrated in Fig. 2: (1) manual selection of the different areas in the micrograph (woven bone, soft tissue, pores, edges) (Fig 2a); (2) manual removal of undesired zones (soft tissue, edges); it should be noted that the colour value of the soft tissue is equal to the colour of the edges and is not considered in estimation of porosity (Fig. 2b, 2c); therefore the region of interest for porosity measurement corresponds with pores and bone tissue areas i.e. non-green areas in Fig. 2d; (3) conversion of the image to greyscale (Fig. 2d); (4) conversion of the image to black and white to be able to distinguish woven bone (white) from pores (black) (Fig. 2e); and, finally, (5) quantification of the porosity.

Fig 2. a) Areas of the mineralised callus identified in the micrographs for the estimation of porosity in the micrograph corresponding to 79 days after surgery; b) delimitation of the callus section; c) region of interest for porosity measurements (non-green areas); d) image conversion to greyscale; e) conversion to black (pores) and white (woven bone).

In step (2), instead of developing an unreliable programme, it was decided to manually modify the micrographs using a freeware image editing programme (GIMP). In each micrograph, the boundary of the callus is carefully analysed, delimited and stained green (RGB, G255), and then eliminated by applying the appropriate colour filter.

In step (4), images are treated as an array of zeros (black) and ones (white) in which each array element symbolises a pixel of the image. The array elements of value 1 correspond to the parts of the callus that are ossified, whereas the elements of value 0 correspond to pores within the callus.

In step (5), the total percentage of porosity in each micrograph is calculated as the ratio of the pores to the total area:

$$Porosity\ (\%) = \frac{Pore\ area}{Total\ area} x100 \quad (1)$$

To analyse the development of the new bone tissue's microarchitecture, the maximum pore area was also automatically calculated. These parameters were evaluated for each micrograph of the distraction callus using the commercial software Matlab® by means of an algorithm based on the function *bwboundaries*. This function traces, within a binary image, all boundaries of independent regions (pores), and areas were quantified to calculate the maximum pore size. The algorithm used allows eliminating any bone islands present within the pores.

The resolution of the micrographs used and the technique applied allow detecting pores from a size of 25 µm in woven bone samples and 6 µm in cortical bone. Therefore, pores with a diameter less than 25 µm in woven bone, and 6 µm in cortical bone, were not taken into account.

The resolution of the micrographs used and the technique applied allow detecting pores from a size of 25 µm in woven bone samples and 6 µm in cortical bone. Therefore, pores with a diameter less than 25 µm in woven bone, and 6 µm in cortical bone, were not taken into account.

Greyscale quantification

To analyse how the bone distraction callus is mineralised, radiographs were examined in terms of their greyscale value. The first step was to select the callus area to be analysed, removing any undesired elements, such as fixator parts (Fig 3). Then, three areas are delimited using the image editor (GIMP): one corresponding to the distraction callus, another to the cortical bone and a third to a 20 x 20 pixel matrix at the upper left-hand corner of the radiograph, taken as a reference (black area surrounded by green lines, Fig. 3c). These three zones are converted to greyscale values by calculating the mean of the pixel values corresponding to the callus ($\overline{Grey}_{callus}$), the cortical bone ($\overline{Grey}_{cortical}$) and the black reference ($\overline{Grey}_{reference}$) and their standard deviation. Afterwards, the percentage of relative mineralisation of the callus with reference to the mineralisation of the cortical bone (greyscale index) is calculated as:

$$Greyscale\ index\ (\%) = \frac{\overline{Grey}_{callus} - \overline{Grey}_{reference}}{\overline{Grey}_{cortical} - \overline{Grey}_{reference}}\ x\ 100 \quad (2)$$

Fig 3. Areas identified in the radiographs for greyscale quantification: (a) initial radiograph, (b) distraction callus and surrounding area and (c) delimited zones within the last area (distraction callus tissue and a 20 x 20 pixel matrix at the upper left-hand corner taken as a reference).

Correlation analysis

The coefficient of determination (R^2) was calculated to analyse the correlation among the variables measured and others measured in previous studies (porosity, greyscale index, Young's Modulus (E) and maximum pore area):

$$R^2 = 1 - \frac{\sum_{i=1}^{n}(Y_i - f_i)^2}{\sum_{i=1}^{n}(Y_i - \bar{Y})^2}, \quad (3)$$

where $f_1 \ldots f_n$ are the predictions by the linear regression of a variable Y associated to the fitted values $Y_1 \ldots Y_n$. $\bar{Y}$ is the mean of the measured and fitted data $\bar{Y} = \frac{1}{n}\sum_{i=1}^{n} Y_i$

5. Results

Porosity in the distraction callus tissue.

Porosity has been measured for samples of woven and cortical bone. The temporal evolution of the porosity of the woven bone within the distraction callus is presented (Fig. 4). For the woven bone, the measured porosity decreases over time. The porosity values of the distraction callus tissue decrease over time approximately 73.3% 35 days after surgery to 31.9% 525 days after surgery. It may be observed that the rate slows down during healing. For example, it decreases 10.2% in 15 days, from day 35 to 50, and 11.4% in 364 days, from day 161 to day 525. The degrees of cortical bone porosity are similar and independent of the sample taken. The mean value and standard deviation of the cortical bone porosity in the samples analysed was 4.1% ± 3.1%. The mean value is included in Fig. 4 for reference, which also shows the maximum pore area for each micrograph, calculated relative to the total callus area.

Fig 4. Porosity values and relative maximum pore area ($Pore_{max}$) in the distraction callus for the different days analysed. Values for the mean porosity of the cortical bone samples are also shown for comparison.

Maximum pore area relative to the total callus area (Fig. 4), evaluated from the micrographs, decreases from 52.0% 35 days after surgery to 6.0% 161 days after surgery. According to the samples analysed, at day 525, maximum pore area in the callus increases again to 16.7%.

Evolution of the greyscale index

The evolution of the greyscale index in the distraction callus tissue is shown in Fig. 5. Each point of this figure represents the value of the greyscale index measured in

radiographs at the time points in Table 2. This value increases up to 60-80% of the greyscale index of the cortical bone, between 70 and 140 days after surgery

Fig. 5: Progression of greyscale index relative to the greyscale index of cortical bone (%) during the bone transport process.

6. Discussion

This study measured the temporal evolution of the porosity as well as the greyscale of woven bone in x-rays. Data showed that the porosity of woven bone can be as much as 80% at the initial stages of the bone transport process (Fig. 4). A similar value for porosity can be found in trabecular bone, with values ranging from 70-95%[35,38]. At the end of bone transport, porosity values measured were much lower (31.9% at 525 days) and tend towards the values measured for cortical bone (4%), which are in concordance with values found in the literature[7] and with data taken from mechanobiological models[5,19-21].

Similar range of values for the woven bone porosity were reported by Vetter et al.[41] in a fracture healing process. However, the level of porosity seems to decrease more rapidly in fracture healing, from 70% to 30% approximately in 49 days, compared to distraction osteogenesis, from 73.3% to 31.9% in 490 days. On the other hand, Mora Macías et al.[32] showed that the woven bone generated during distraction osteogenesis seems to present a similar temporal evolution of the elastic modulus than fracture healing[24]. Therefore, it could be concluded that the particularities in the evolution of the ossification of the distraction osteogenesis callus[23] affect the evolution of the woven bone microarchitecture and therefore its macroscopic stiffness despite presenting a similar evolution of the elastic modulus than fracture healing.

In silico studies published in the literature use a constant value for the porosity of immature bone: 80%[5,19-21]. As can be seen in Fig 4, the initial porosity measured in this study, corresponding to day 35 after surgery, is very close to this value: 73.3%. However, as the bone healing process takes place, the percentage of porosity decreases considerably, especially during the first few days of the study, and rapidly deviates from the values used in *in silico* models, which were considered constant throughout the process. Thus, the constant value of 80% porosity used in the literature does not seem to be adequate for modelling the development of the mechanical properties of the woven bone during the complete healing process. Porosity of the woven bone must be considered in computational models of the bone regeneration processes, especially after bony bridging, as showed Vetter et al.[42] and Mora-Macías et al.[33].

Pore area analysis (Fig. 4) shows that the high values of porosity in the initial stages of the consolidation period may be due to a large average pore area. This can also be observed in Fig. 6, which shows the pore distribution (black areas) in the micrographs from 35 and 525 days after surgery. The high interconnectivity existing in the initial stages of healing (Fig. 6) explains the high values of the maximum pore area during the first 100 days after surgery. In addition, it can be observed in Fig 4 that the maximum pore area increases from day 161 to day 565 (up to 3 times). This may be due to the fact that the pores of the woven bone in the distraction callus may be regrouped. The pore area might increase during the last stages of the process due to the re-establishment of the medullary cavity (Fig. 6b), as by day 525 intense remodelling activity has already taken place[28]. Although the reported evolution between 161 and 525 days after surgery should be taken with caution because, with one sample per time point, it could also be due to interindividual differences.

Fig. 6: Pore distribution (black areas) in the micrographs from a) 35 and b) 525 days. Blue line represents the border of the pore with the greatest area.

The greyscale index at the end of the experiment (Fig. 5) is between 50-60%, below the peak values reached 70-140 days after surgery. A greyscale index of 100% would imply that the bone sample being studied has been totally remodelled into cortical bone. It may be observed that the temporal progression of the greyscale index follows a similar trend than the temporal progression of the volume of the callus measured in previous studies[28]. Both reached a peak between 70 and 140 days after surgery. After this, the greyscale index decreased. The authors think that this decrease in the greyscale index is due to the development of the medullary cavity[28], which is a large area with no mineral content. Therefore, the greyscale index after reaching the peak value may not be considered a good indicator of the evolution of the mean mineral content of the callus.

The relationship between the elastic modulus of the woven bone (E), the porosity and the greyscale index is shown in Fig. 7. There is an inverse linear correlation between the porosity and the greyscale index of the bone distraction callus (R^2= 0.864) according to Fig. 7a. Inverse linear correlation may be observed (Fig 7b) between the elastic modulus of the woven bone measured in a previous study[32] and the porosity (R^2=0.927). As the consolidation phase takes place, the porosity decreases and the greyscale index increases, as has been proven in previous studies of cortical bone[2,8,9,11,38]: the greater the porosity, the lower the stiffness and vice versa. In addition, the relationship between the Young's modulus and the greyscale index (Fig. 7c) shows that there is a strong relationship (R^2= 0.777): the greater the greyscale index, the greater the Young's modulus, which is also in accordance with data from the literature[7,24]. Finally, it can also be observed in Fig. 7d that the maximum area of the pores is also correlated with the percentage of porosity (R^2=

0.735). Therefore, it seems that the microarchitecture of the woven bone becomes more compact by means of reducing both porosity and the pore area.

Fig. 7. Relationships between porosity, greyscale index, Young's Modulus (E) and maximum pore area. (a) Mean greyscale of the week corresponding to the time point when porosity was measured versus porosity level. (b) E versus porosity. (c) E versus mean greyscale of the week corresponding to the time point when E was measured. (d) Maximum pore versus porosity level. E data were measured in a previous work[32]. Note that a and c show only 5 experimental points because the radiography study ended 374 days after surgery; however, porosity and E were evaluated once more at 525 days after surgery.

There are several limitations in the present study. Firstly, in order to calculate the porosity it has been assumed that pores correspond to the black regions, although soft tissue could also be located in these areas. In addition, pores with a diameter of less than 25 μm were not taken into account in porosity measurements of woven bone samples, 6 μm in the case of cortical bone ones. Secondly, the study carried out has been developed in two dimensions. Finally, the need to use different animals for each time point introduces a source of variation in the porosity measurements. Therefore, future studies with a higher number of samples per time point will be valuable to make stronger conclusions.

To the authors' knowledge, the dependence of the mechanical properties of woven bone on its microarchitecture and especially on its porosity and greyscale has not yet been analysed. In this work, *ex vivo* samples, as well as radiographs, have been used to measure both porosity and greyscale. The second could be related to the mineral content of the woven bone. Therefore, the results of this study may contribute to the development of micromechanical models of woven bone and improvements in *in silico* modelling.

However, this is a preliminary study. Further three-dimensional works, as well as a larger number of samples to be analysed, are needed to completely corroborate the data.

7. Acknowledgments

The authors gratefully acknowledge the Ministerio de Economía y Competitividad del Gobierno España (grant number DPI2017-82501-P) and the Consejería de Innovación, Ciencia y Empleo de la Junta de Andalucía (grant numbers P09-TEP-5195 and US-1261691) for research funding.

8. Conflict of interest

The authors have no conflict of interest to disclose.

9. References

[1] Aldieri A, Terzini M, Osella G, Priola AM, Angeli A, Veltri A, et al. Osteoporotic hip fracture prediction: is T-score based criterion enough? A Hip Structural Analysis based model. J Biomech Eng. doi: 10.1115/1.4040586, 2018

[2] Augat P, Claes LE. Prediction of fracture load at different skeletal sites by geometric properties of the cortical shell. J. Bone Miner. Res. 11: 1356–63, 1996

[3] Boccaccio A, Prendergast PJ, Pappalettere C, Kelly DJ. Tissue differentiation and bone regeneration in an osteotomized mandible: a computational analysis of the latency period. Med. Biol. Eng. Comput. 46: 283–98, 2008.

[4] Brunner UH1, Cordey J, Schweiberer L, Perren SM. Force required for bone segment transport in the treatment of large bone defects using medullary nail fixation. Clin Orthop Relat Res, (301):147-55, 1994.

[5] Burke DP, Kelly DJ. Substrate stiffness and oxygen as regulators of stem cell differentiation during skeletal tissue regeneration: a mechanobiological model. PLoS One. 7: e40737, 2012

[6] Claes LE, Laule J, Wenger K, Suger G, Liener U, Kinzl L. The influence of stiffness of the fixator on maturation of callus after segmental transport. J. Bone Jt. Surg. Br. 82: 142–148, 2000

[7] Currey JD. The relationship between the stiffness and the mineral content of bone. J Biomech. 2: 477–80, 1969

[8] Currey JD. Changes in the impact energy absorption of bone with age. J. Biomech. 12: 459–69, 1979.

[9] Currey JD. The effect of porosity and mineral content on the Young's modulus of elasticity of compact bone. J. Biomech. 21: 131–9, 1988.

[10] Currey JD. Bones: Structure and Mechanics. Princeton University Press, Princeton, 2002.

[11] Currey JD. Incompatible mechanical properties in compact bone. J. Theor. Biol. 231: 569–80, 2004.

[12] Currey JD, Shahar R. Cavities in the compact bone in tetrapods and fish and their effect on mechanical properties. J. Struct. Biol. 183: 107–22, 2013.

[13] Dahl MT, Gulli B, Berg T. Complications of limb lengthening. A learning curve. Clin. Orthop. Relat. Res. 301: 10–8, 1994.

[14] Floerkemeier T, Thorey F, Hurschler C, Wellmann M, Witte F, Windhagen H. Stiffness of callus tissue during distraction osteogenesis. Orthop. Traumatol. Surg. Res. 96: 155–160, 2010.

[15] Fürmetz J, Soo C, Behrendt W, Thaller PH, Siekmann H, Böhme J, Josten C. Bone Transport for Limb Reconstruction Following Severe Tibial Fractures. Orthop Rev (Pavia), 31;8(1):6384, 2016.

[16] Gong JK, Arnold JS, Cohn SH. The density of organic and volatile and non-volatile inorganic components of bone. Anat. Re. 149: 319-324, 1964.

[17] Ilizarov GA. The tension-stress effect on the genesis and growth of tissues: Part II. The influence of the rate and frequency of distraction. Clin Orthop Relat Res, (239):263-85,1989.

[18] Ilizarov GA. The tension-stress effect on the genesis and growth of tissues. Part I. The influence of stability of fixation and soft-tissue preservation. Clin Orthop Relat Res, (238):249-81, 1989.

[19] Isaksson H, Comas O, van Donkelaar CC, Mediavilla J, Wilson W, Huiskes R et al. Bone regeneration during distraction osteogenesis: mechano-regulation by shear strain and fluid velocity. J. Biomech, 40: 2002–2011, 2007

[20] Isaksson H, van Donkelaar CC, Huiskes R, Ito K. A mechano-regulatory bone-healing model incorporating cell-phenotype specific activity. J. Theor. Biol. 252: 230–246, 2008

[21] Lacroix D, Prendergast P. A mechano-regulation model for tissue differentiation during fracture healing: analysis of gap size and loading. J. Biomech. 35: 1163–1171, 2002

[22] Leong PL, Morgan EF. Correlations between indentation modulus and mineral density in bone-fracture calluses. Integr. Comp. Biol. 49: 59-68, 2009

[23] López-Pliego EM, Giráldez-Sánchez MÁ, Mora-Macías J, Reina-Romo E, Domínguez J. Histological evolution of the regenerate during bone transport: an experimental study in sheep. Injury, 47 Suppl 3:S7-S14, 2016.

[24] Manjubala I, Liu Y, Epari DR, Roschger P, Schell H, Fratzl P et al. Spatial and temporal variations of mechanical properties and mineral content of the external callus during bone healing. Bone. 45: 185-92, 2009.

[25] Martin B. Aging and strength of bone as a structural material. Calcif. Tissue Int. 53: S34–39, 1993.

[26] Martínez-Reina J, García-Rodríguez J, Mora-Macías J, Domínguez J, Reina-Romo E. Comparison of the volumetric composition of lamellar bone and the woven bone of calluses. Proc. Inst. Mech. Eng. H. 232: 682-689, 2018

[27] McCalden RW, McGeough JA, Barker MB, Court-Brown CM. Age-related changes in the tensile properties of cortical bone. The relative importance of changes in porosity, mineralization, and microstructure. J. Bone Joint Surg. Am. 75: 1193–1205, 1993.

[28] Mora-Macías J., Reina-Romo E, López-Pliego M, Giráldez-Sánchez MA, Domínguez J. In vivo mechanical characterization of the distraction callus during bone consolidation. Ann. Biomed. Eng. 43: 2663–2674, 2015.

[29] Mora-Macías J, Reina-Romo E, Domínguez J. Distraction osteogenesis device to estimate the axial stiffness of the callus in vivo. Med. Eng. Phys. 37: 969–978, 2015

[30] Mora-Macías J, Reina-Romo E, Morgaz J, Domínguez J. In vivo gait analysis during bone transport. Ann. Biomed. Eng. 43: 2090–2100, 2015

[31] Mora-Macías J., Reina-Romo E, Domínguez J. Model of the distraction callus tissue behavior during bone transport based in experiments in vivo. J. Mech. Behav. Biomed. Mater. 61: 419–430, 2016.

[32] Mora-Macías J, Pajares A, Miranda P, Domínguez J, Reina-Romo E. Mechanical characterization via nanoindentation of the woven bone developed during bone transport. J. Mech. Behav. Biomed. Mater. 74: 236–244, 2017

[33] Mora-Macías J, Giráldez-Sánchez MA, López M, Domínguez J, Reina-Romo E. Comparison of methods for assigning the material properties of the distraction callus in computational models. Int J Numer Method Biomed Eng. 35(9), e3227, 2019

[34] Papakostidis C1, Bhandari M, Giannoudis PV. Distraction osteogenesis in the treatment of long bone defects of the lower limbs: effectiveness, complications and clinical results; a systematic review and meta-analysis. Bone Joint J, 95-B(12):1673-80, 2013.

[35] Renders GAP, Mulder L, van Ruijven LJ, van Eijden TMGJ. Porosity of human mandibular condylar bone. J. Anat. 210: 239–248, 2007.

[36] Richardson SS, Schairer, WW, Fragomen AT, Rozbruch SR. Cost Comparison of Femoral Distraction Osteogenesis With External Lengthening Over a Nail Versus Internal Magnetic Lengthening Nail. Journal of the American Academy of Orthopaedic Surgeons, Volume 27 - Issue 9 - p e430-e436, 2019.

[37] Roschger P, Fratzl P, Eschberger J, Klaushofer K. Validation of quantitative backscattered electron imaging for the measurement of mineral density distribution in human bone biopsies. Bone. 23: 319–26, 1998

[38] Schaffler MB, Burr DB. Stiffness of compact bone: effects of porosity and density. J. Biomech. 21: 13–16, 1988.

[39] Shen Z, Lin H, Chen G, Zhang Y, Li Z, Li D, Xie L, Li Y, Huang F, Jiang Z. Comparison between the induced membrane technique and distraction

osteogenesis in treating segmental bone defects: An experimental study in a rat model. PLoS One, 20;14(12), 2019.

[40] Shefelbine SJ, Simon U, Claes L, Gold A, Gabet Y, Bab I et al. Prediction of fracture callus mechanical properties using micro-CT images and voxel-based finite element analysis. Bone. 36: 480–8, 2005.

[41] Vetter A, Liu Y, Witt F, Manjubala I, Sander O, Epari DR, Fratzl P, Duda GN, Weinkamer R. The mechanical heterogeneity of the hard callus influences local tissue strains during bone healing: a finite element study based on sheep experiments. J Biomech. 44(3):517-23, 2011.

[42] Vetter A, Epari DR, Seidel R, Schell H, Fratzl P, Duda GN, Weinkamer R. Temporal tissue patterns in bone healing of sheep. J Orthop Res, 28(11):1440-7, 2010.

[43] Wachter NJ, Krischak GD, Mentzel M, Sarkar MR, Ebinger T, Kinzl L et al. Correlation of boneineral densitywith strength and microstructural parameters of cortical bone in vitro. Bone. 31: 90–95, 2002

[44] Zanetti EM, Bignardi C. Structural analysis of skeletal body elements: Numerical and experimental methods. In C. T. Leondes (Ed.), Biomechanical Systems Technology: Muscular Skeletal Systems (pp. 185-225), 2009

10. Tables, figure and legends

Authors	*Application*	$E_{immature\ bone}$ *(MPa)*	*Porosity Immature bone (%)*	$E_{cortical\ bone}$ *(MPa)*	*Porosity Cortical bone (%)*
Lacroix & Prendergast [29]	Tissue differentiation	1000	80	20000	4
Isaksson et al. [30,31]	Bone regeneration	1000	80	15750	4
Boccaccio et al [34]	Bone regeneration	1000	80	20000	-
Burke & Kelly [32]	Cell differentiation	1000	80	20000	4

Table 1: Values for the porosity and Young's modulus (E) of the woven and cortical bone used in mechanobiological models

Sheep	Time points evaluated (days from surgery)
1	10, 16, 24, 31, 38, 51, 64, 72, 83, 98
2	7, 23, 30, 37, 44, 52, 66, 79
3	7, 21, 28, 34
4	8, 21, 28, 35, 42, 49, 64, 80, 94, 128, 154
5	7, 22, 29, 37, 45, 56, 70, 100, 130, 143, 150, 176, 192, 206, 220, 247, 277, 311, 343, 374
6	7, 21, 28, 36
7	9, 21
8	8, 22, 29
9	17
10	10, 21, 28, 35, 42, 49, 57, 74, 80, 101, 107, 137, 171, 203, 234
11	7, 22, 29, 36, 43, 52

Table 2. Time points at which radiographs were taken of each of the 11 sheep in the study

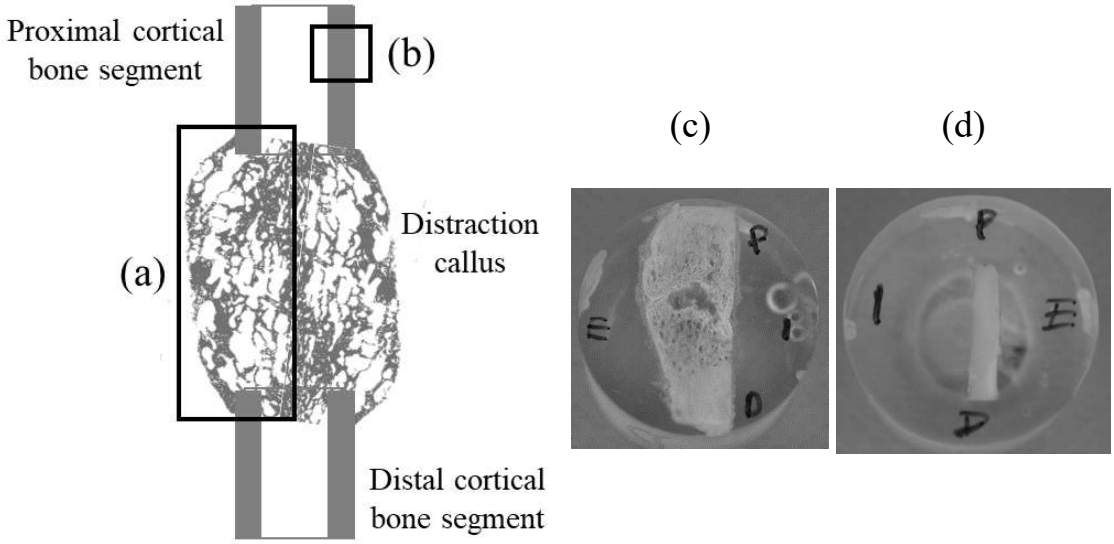

Fig. 1.Location of the (a) distraction callus and (b) cortical bone samples within the cross section (parallel to frontal plane) of the intervened metatarsus. Photographs shown in (c) and (d) correspond to the distraction callus and cortical bone samples respectively taken from the sheep sacrificed at day 79 after surgery.

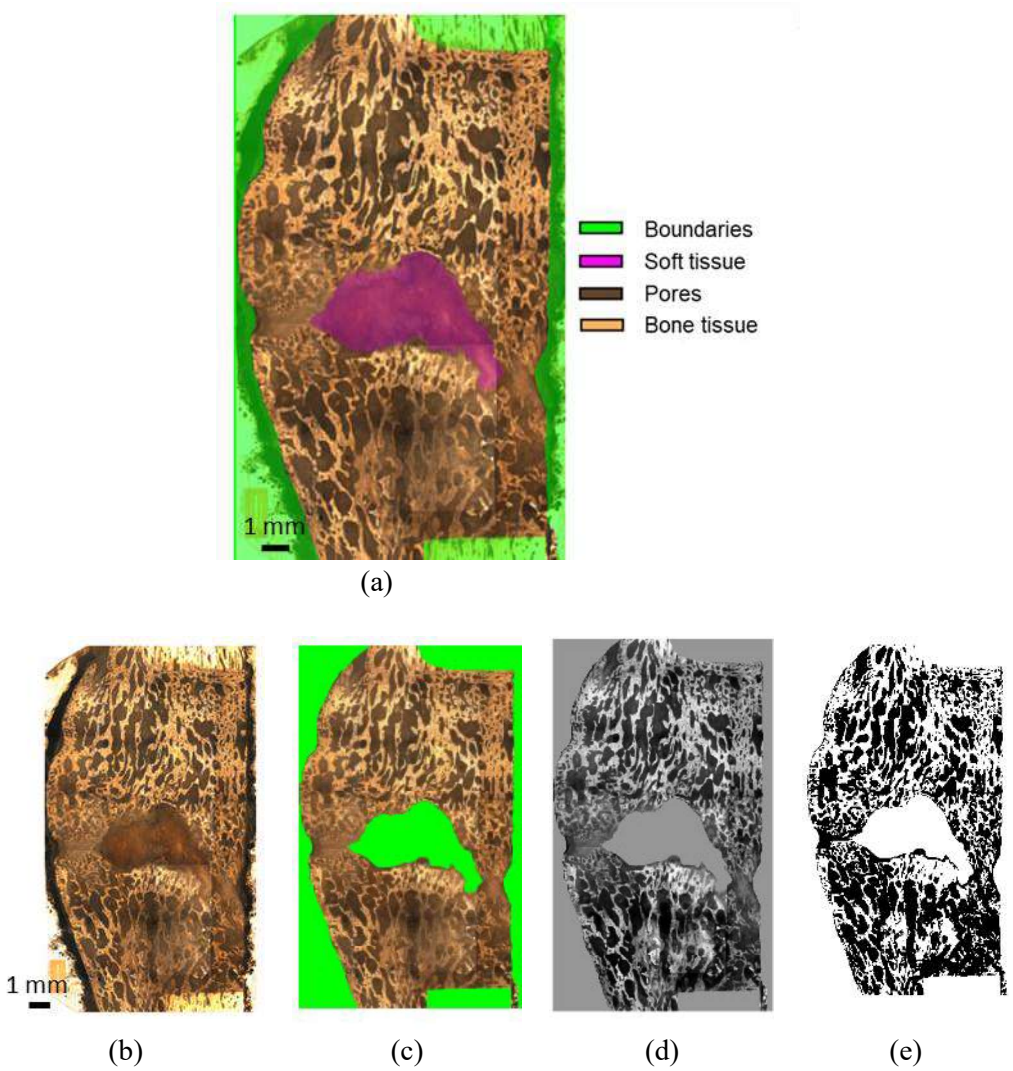

Fig. 2. a) Areas of the mineralised callus identified in the micrographs for the estimation of porosity, in the micrograph corresponding to 79 days after surgery; b) delimitation of the callus section; c) region of interest for porosity measurements (non-green areas); d) image conversion to greyscale; e) conversion to black (pores) and white (woven bone).

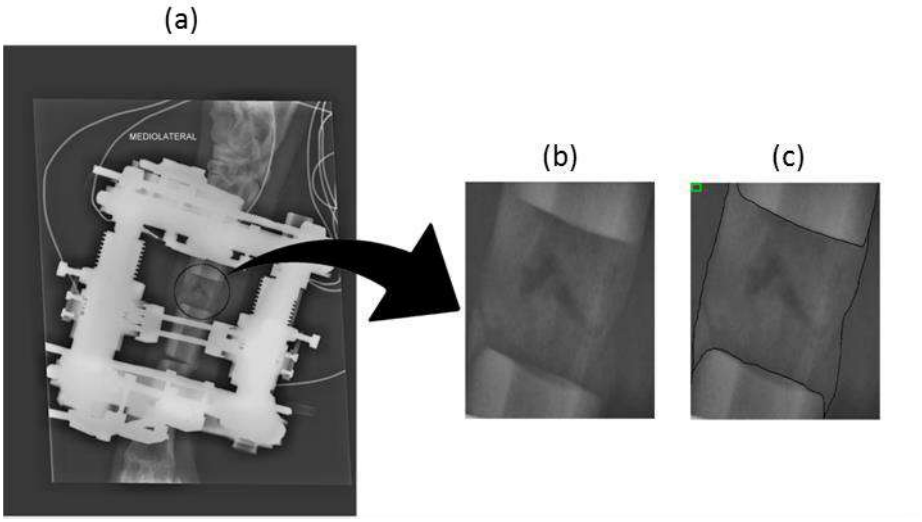

Fig. 3. Areas identified in the radiographs for greyscale quantification: (a) initial radiograph, (b) distraction callus and surrounding area and (c) delimited zones within the last area (distraction callus tissue and a 20 x 20 pixel matrix at the upper left-hand corner taken as a reference).

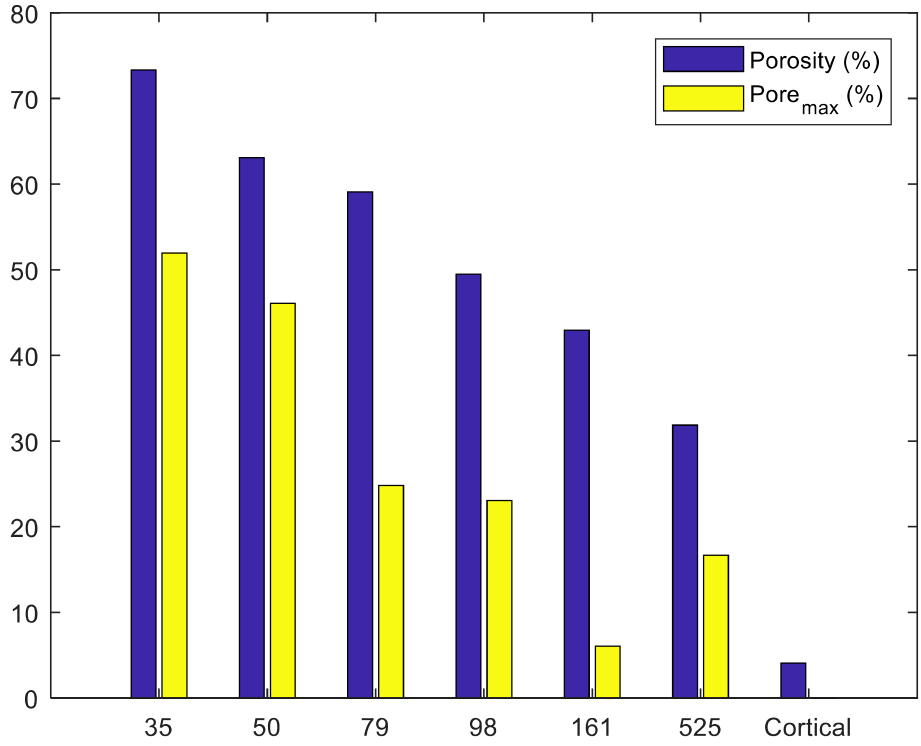

Fig. 4. Porosity values and relative maximum pore area ($Pore_{max}$) in the distraction callus for the different days analysed. Values for the mean porosity of the cortical bone samples are also shown for comparison.

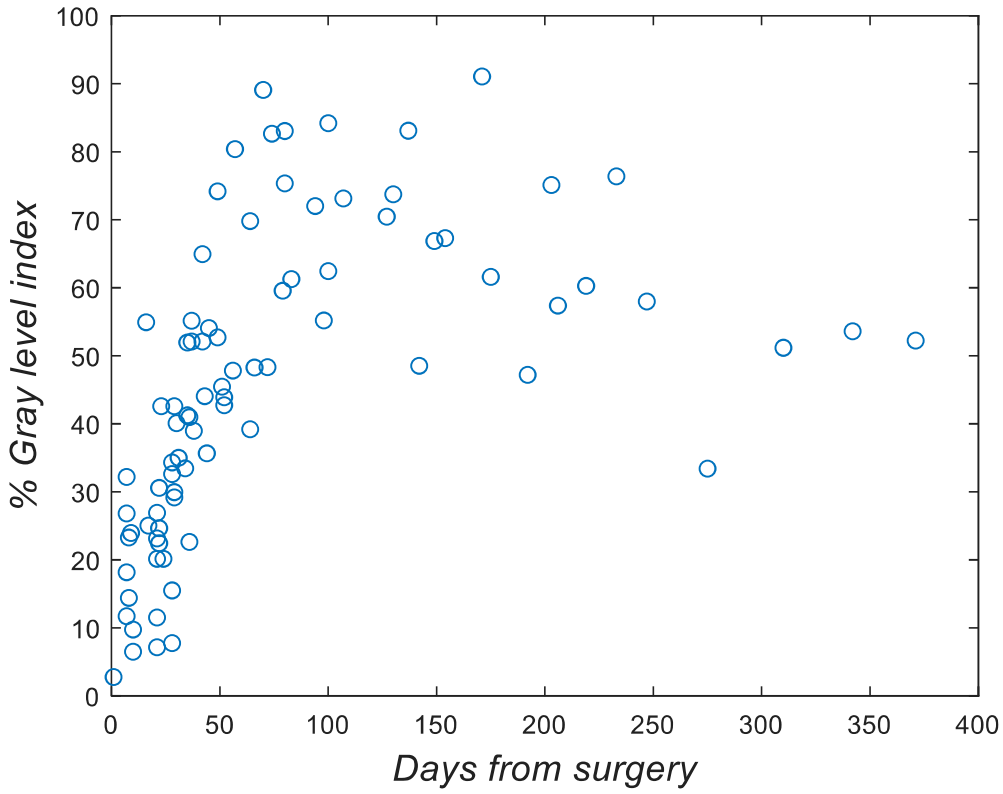

Fig. 5: Progression of greyscale index relative to the greyscale index of cortical bone (%) during the bone transport process.

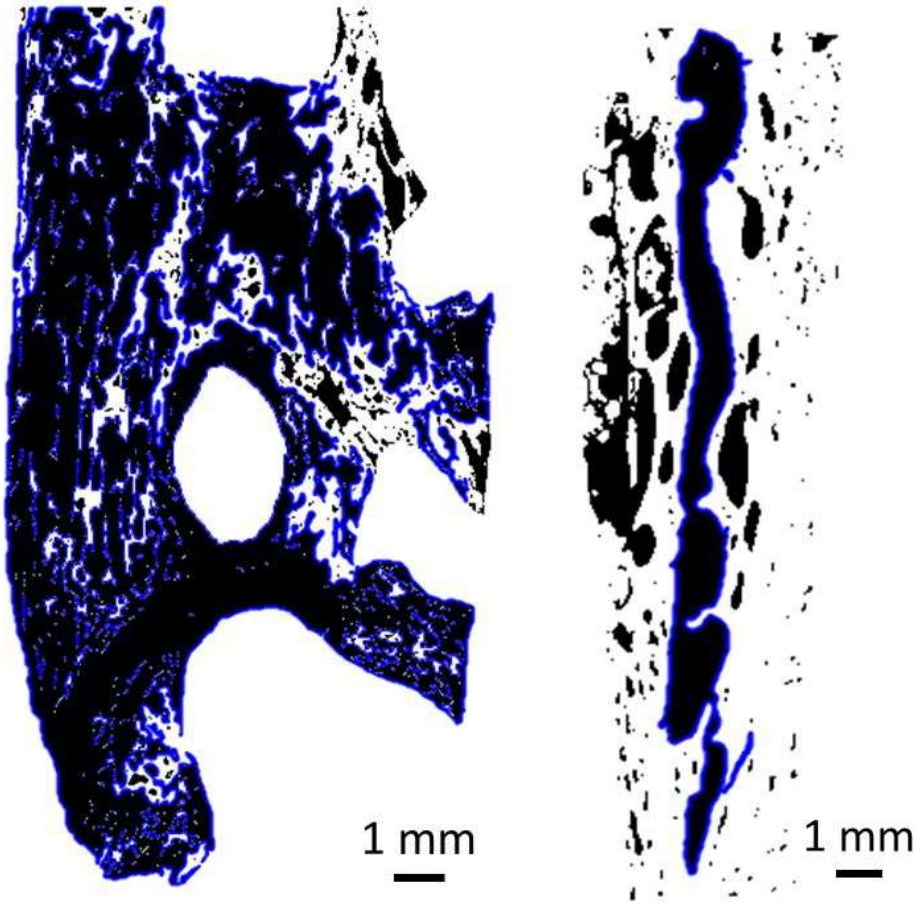

(a) (b)

Fig. 6: Pore distribution (black areas) in the micrographs from a) 35 and b) 525 days. Blue line represents the border of the pore with the greatest area.

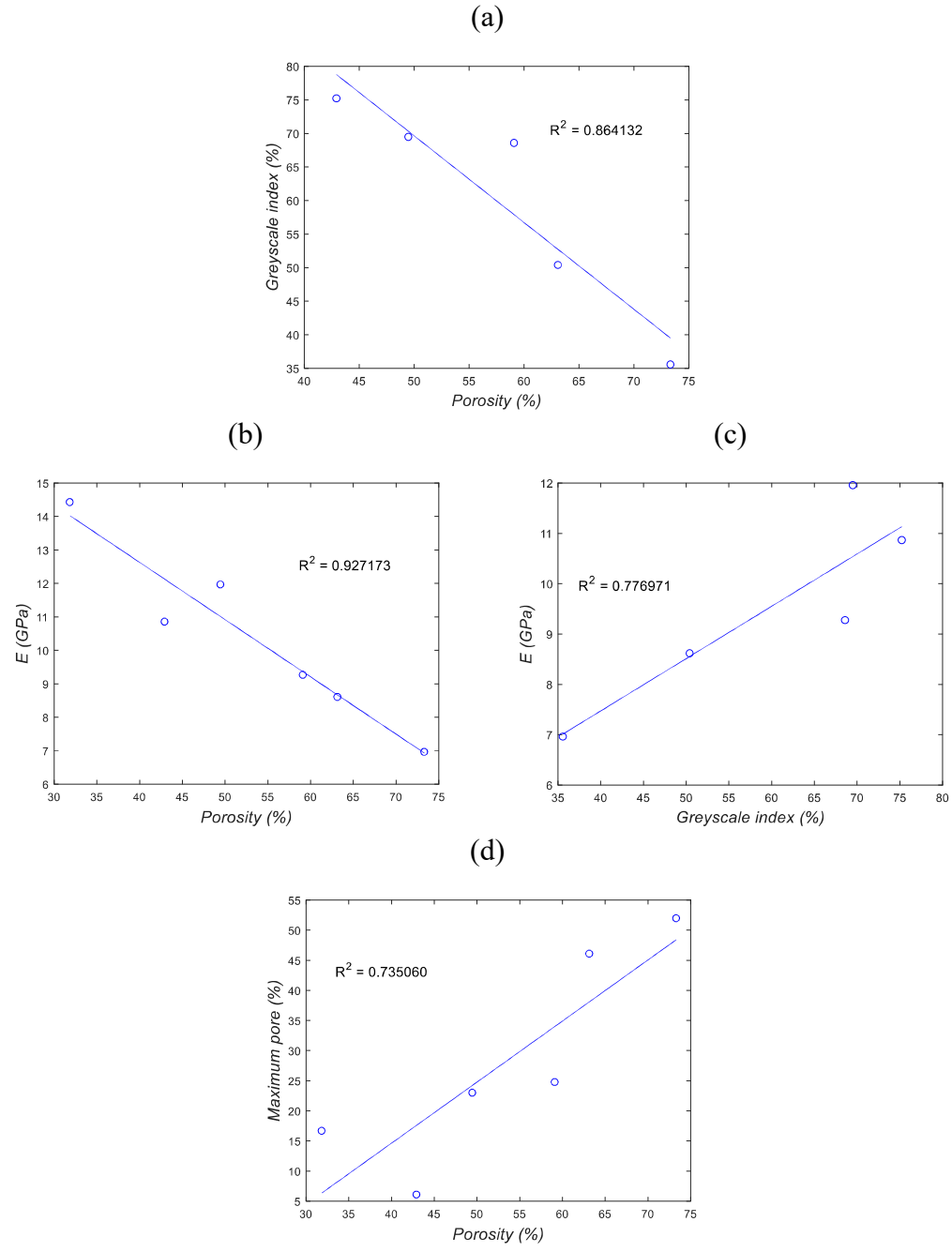

Fig. 7. Relationships between porosity, greyscale index ~~level~~, Young's Modulus (E) and maximum pore area. (a) Mean greyscale of the week corresponding to the time point when porosity was measured versus porosity level. (b) E versus porosity. (c) E versus mean greyscale of the week corresponding to the time point when E was measured. (d) Maximum pore versus porosity level. E data were measured in a previous work[32]. Note that a and c show only 5 experimental points because the radiography study ended 374

days after surgery; however, porosity and E were evaluated once more at 525 days after surgery.